

AD-E410617

12

AD

AD A123365

CHEMICAL SYSTEMS LABORATORY CONTRACTOR REPORT

ARCSL-CR-82028

INFRARED EMISSION FROM GAS-AEROSOL REACTIONS

by

Raymond A. Mackay

September 1982

Department of Chemistry
Drexel University
Philadelphia, Pennsylvania 19104

Contract No. DAAK11-80-C-0051

DTIC
ELECTE
JAN 3 1983
S D
B



US ARMY ARMAMENT RESEARCH AND DEVELOPMENT COMMAND
Chemical Systems Laboratory
Aberdeen Proving Ground, Maryland 21010



Approved for public release; distribution unlimited.

82 12 14 002

DTIC FILE COPY

Disclaimer

The views, opinions, and/or findings contained in this report are those of the authors and should not be construed as an official Department of the Army position, policy, or decision unless so designated by other documentation.

Disposition

Destroy this report when it is no longer needed. Do not return it to the originator.

UNCLASSIFIED

SECURITY CLASSIFICATION OF THIS PAGE (When Data Entered)

REPORT DOCUMENTATION PAGE		READ INSTRUCTIONS BEFORE COMPLETING FORM
1. REPORT NUMBER ARCSL-CR-82028	2. GOVT ACCESSION NO. AD-A123365	3. RECIPIENT'S CATALOG NUMBER
4. TITLE (and Subtitle) INFRARED EMISSION FROM GAS-AEROSOL REACTIONS		5. TYPE OF REPORT & PERIOD COVERED TECHNICAL REPORT 7/1/80 - 6/30/82
		6. PERFORMING ORG. REPORT NUMBER
7. AUTHOR(s) RAYMOND A. MACKAY		8. CONTRACT OR GRANT NUMBER(s) DAAK11-80-C-0051
9. PERFORMING ORGANIZATION NAME AND ADDRESS Department of Chemistry Drexel University Philadelphia, Pa. 19104		10. PROGRAM ELEMENT PROJECT, TASK AREA & WORK UNIT NUMBERS 1L161102A71A-D
11. CONTROLLING OFFICE NAME AND ADDRESS Commander, Chemical System Laboratory ATTN: DRDAR-CLJ-R Aberdeen Proving Ground, MD. 21010		12. REPORT DATE September 1982
		13. NUMBER OF PAGES 38
14. MONITORING AGENCY NAME & ADDRESS (if different from Controlling Office) Commander, Chemical System Laboratory ATTN: DRDAR-CLB-PS Aberdeen Proving Ground, MD. 21010		15. SECURITY CLASS. (of this report) UNCLASSIFIED
		15a. DECLASSIFICATION DOWNGRADING SCHEDULE NA
16. DISTRIBUTION STATEMENT (of this Report) Approved for public release; distribution unlimited.		
17. DISTRIBUTION STATEMENT (of the abstract entered in Block 20, if different from Report)		
18. SUPPLEMENTARY NOTES This investigation was sponsored by the Army Smoke Research Program Chemical System Laboratory, Aberdeen Proving Ground, MD. Contract Project Officer: Dr. Edward W. Stuebing DRDAR-CLB-PS (301) 671-3089		
19. KEY WORDS (Continue on reverse side if necessary and identify by block number)		
Infrared Emission	Gaseous Amonia	Infrared (IR)
Gas-aerosol Reactions	Sulfuric Acid-amonia	IR Luminescence
Exothermic Reactions	Octanoic Acid-amonia	IR Laser
Acid-base Reactions	Octylamine-hydrogen Chloride	Thermal Emission
Chlorosulfonic Acid Aerosol	Spectral Radiance	Volatile Co-aerosol
20. ABSTRACT (Continue on reverse side if necessary and identify by block number) The present investigation has been designed to produce infrared emission by means of an exothermic reaction between a liquid aerosol and a gas. A number of gas-aerosol systems employing acid-base reactions have been examined and significant levels of radiation observed from the reactions of chloro-sulfuric acid aerosol with gaseous amonia and water. Other systems which were screened including sulfuric acid-ammonia, octanoic acid-ammonia, and octylamine-hydrogen chloride, have produced detectable levels of radiation. Some methods		

DD FORM 1473
1 JAN 73

UNCLASSIFIED

SECURITY CLASSIFICATION OF THIS PAGE (When Data Entered)

UNCLASSIFIED

CLASSIFICATION OF THIS PAGE (When Data Entered)

20. ABSTRACT (Continued)

for the investigation of emission from the gas-aerosol reactions have been explored, and the results of these studies utilizing a chlorosulfonic-acid aerosol system are presented.

UNCLASSIFIED

PREFACE

The work reported herein was authorized by Contract DAAK11-80-C-0051, INFRARED EMISSION FROM GAS-AEROSOL REACTIONS. The work was performed from Department of Chemistry, Drexel University, Philadelphia, Pa. 19104

The use of trade names in this report does not constitute an official endorsement or approval of the use of such commercial hardware or software. This report may not be cited for purposes of advertisement.

Reproduction of this document in whole or in part is prohibited except with permission of Commander, Chemical Systems Laboratory, ATTN: DRDAR-CLJ-R, Aberdeen Proving Ground, Maryland 21010. However, the Defense Technical Information Center and the National Technical Information Service are authorized to reproduce the document for United States Government purposes.

Acknowledgments

I wish to acknowledge the contributions of Mr. K. Heaps, Ms. G. Dalickas, Mr. R. Fischer, and Mr. M. Suresh to various portions of the experimental work. I also wish to thank Dr. C. Acquista for many valuable discussions, and the U.S. Army Research Office and the Chemical Systems Laboratory, Aberdeen Proving Ground for financial support.



Accession For	
NTIS GRA&I	<input checked="checked" type="checkbox"/>
DTIC TAB	<input type="checkbox"/>
Unannounced	<input type="checkbox"/>
Justification	
By	
Distribution/	
Availability Codes	
Dist	Avail and/or Special
A	

Contents

	Page
1. INTRODUCTION	7
2. RESULTS AND DISCUSSION	9
2.1 Aerosol Generation and Detection	9
2.2 Gas-Aerosol Reactions	11
2.3 Temperature-Distance Profiles	13
2.4 Emittance-Temperature Profiles	15
3. CONCLUSION	18
REFERENCES	19
APPENDIX. List of Figures	21
DISTRIBUTION LIST	33

INFRARED EMISSION FROM GAS-AEROSOL REACTIONS

I. INTRODUCTION

Infrared radiation in the atmosphere above normal background levels can be produced in a variety of ways. For example, combustion gases¹ can produce significant amounts of radiation in the infrared region (2 to 20 μ m). However, the total mass of material, and thus the radiant emittance, is small. In addition, the gas cloud rapidly cools and disperses. In order to significantly increase the amount of airborne material, an aerosol must be employed.

At ambient temperatures (25°C) the maximum of the blackbody emission curve is at about 1030 cm^{-1} ($9.7\mu\text{m}$), which means that a few degrees increase in temperature will produce an increase in spectral radiance on the order of 5% at 5 to $10\mu\text{m}$. A highly conducting and absorbing substance may approximate a blackbody, but most real aerosol particles will at best be "grey" bodies with perhaps some superimposed structure (selectivity). The (equilibrium) thermal emittance of an aerosol particle will therefore be less than that of a blackbody at the same temperature, according to Kirchhoff's Law. A second and more selective method could involve the production of infrared fluorescence. This would have the advantage of being selective as to wavelength range and would thus also require much less total energy input. Unfortunately, due to the rapidity with which vibrational energy degrades, it does not seem possible to employ this approach. In other words, in order to obtain infrared (IR) luminescence in any observable yield, a dilute gas and a high energy IR laser is normally required. We have therefore focused attention on thermal

emission.

In order to accomplish the desired goal, an exothermic chemical reaction must be employed to raise the temperature of the aerosol particle above ambient. This reaction must ultimately involve either the reaction of a gas with the aerosol or the simultaneous generation of a very highly disperse co-aerosol which will rapidly coagulate with the coarser aerosol and react. This is technically more difficult, and there would always be the problem of the highly disperse aerosol coagulating with itself. In the former case, the gas could be generated as a volatile co-aerosol.

A large number of chemical reaction studies have been performed on the upper end of the particle size spectrum with regard to the combustion of fuel sprays and dust clouds². These involve particles in the super-micron range (10 to 1000 μ m). Chemical reactions responsible for heterogeneous nucleation have also been investigated,³⁻⁵ and the particle sizes here are below 0.1 μ m. However, once aerosols are produced either by nucleation and growth in the atmosphere or by nebulization followed by settling and coagulation, most of these achieve a relatively stable existence in the 0.1 to 10 μ m range as smokes, fogs, etc.^{6,7} These systems are polydisperse, with number densities generally less than 10⁷cm⁻³. Nonetheless, there have been relatively few studies of the reactions of gases with aerosol particles in this size regime.

In principle, the reaction rate may be controlled by gas phase diffusion, diffusion of reactants and/or products in the particle, by the bulk chemical reaction, or by processes occurring in the droplet interface region. Cadle and Robbins⁸ have developed equations for some limiting cases and applied them to the reaction of ammonia with sulfuric acid aerosols in the 0.2 to 0.9 μ m range, and to the reaction of NO₂ with a sodium chloride aerosol. In the former case, it was suggested that the rates in concentrated H₂SO₄

droplets, the rate was too fast to measure on their apparatus, and it was presumed that the rate was controlled by gas phase diffusion.^{8,9}

There have also been a number of studies of the metal-catalyzed oxidation of SO_2 in aqueous aerosols. Johnstone and Coughanour¹⁰ using a suspended 500 to 1000 μm drop, concluded that the reaction was liquid-phase controlled with all of the reaction occurring in the outer shell at high manganese concentration. At lower catalyst concentration, the SO_2 penetrated to the center of the drop. The oxidation of SO_2 in 100 to 1000 μ aqueous ammonia drops was also controlled by liquid phase diffusion.¹¹ However, extrapolation of the manganese catalyzed oxidation rates in the supermicron drop to an atmospheric fog of 20 μm droplets predicted a rate 500 times that observed.¹²

Because of the importance of atmospheric reactions,¹³ studies have focused on water droplets and reactions involving SO_2 , NO_2 , NH_3 , H_2SO_4 , and various metal salts. In these cases, the frequently complex reactions are generally also accompanied by droplet growth. This is not the case in the well-controlled reaction of submicron sized 1-octadecene droplets with bromine gas.¹⁴ However, this reaction is slow and not highly exothermic. Nonetheless, these studies do indicate that it should be possible to produce thermal emission as a result of a gas-aerosol reaction, and we report here the results of initial investigations utilizing exothermic reactions between gases and liquid aerosols.

2. RESULTS AND DISCUSSION

2.1 Aerosol Generation and Detection.

For these initial studies, the aerosols were generated by means of a

compressed air nebulizer (DeVilbiss). This generator produces an aerosol with a wide distribution of sizes (i.e. - polydisperse) and with a mass median diameter generally in the range of 2 to $4\mu\text{m}$, depending upon the liquid. However, this generator is easy to employ, and the mass concentration of the aerosol is quite reproducible under the same conditions of flow rate and tank pressure. Nitrogen gas (20 psi) at a flow rate of 3 to 6 l/min was employed, resulting in a reproducibility of about 5% for sulfuric acid and dibutylphthalate (DBP).

All of the studies reported here have been carried out in the reaction tubes shown in Figure A-1. The wall-less tube (Figure A-1a) will be referred to as the "open" tube, and the other (Figure A-1b) as the "closed" tube. In both tubes the reactive gas stream emerges from the inner tube, the aerosol from the next concentric tube, and the sheathing gas from the outer tube. The principal modifications from earlier designs are the mixing of reactive gas with aerosol via small holes at right angles to the aerosol flow rather than through a glass frit and, for the closed tube, the use of a larger (~ 2.5 cm diameter) radiometer viewing port. The reaction tube, radiometer and exhaust are mounted in a metal frame shown schematically in Figure A-2. The entire setup is in a hood, but the exhaust fans in the hood cannot be used since the vibrations and airflow patterns cause excessive interference with the radiometer. For the open tube, a configuration employing a 4 inch diameter exhaust hose and auxiliary fan located outside the hood has proved effective. Arrangements involving cone-shaped vacuum exhausts were not effective. The radiometer is on a traverse for accurate and reproducible positioning, and thermistor probes may be inserted in the gas stream at variable locations.

The radiometer is a Molelectron pyroelectric radiometer model PR200 with a response time of 3 sec for $20\mu\text{W cm}^{-2}$ full scale, a 0.1 Sr field of view, and

a detector area of 0.2 cm^2 . The closed tube and the radiometer are fitted with a KRS-5 window which has a cutoff at about 50μ . Thus, essentially all of the emitted radiation is collected. The thermistor probes (YSI series 400) have a time response of 4 to 5 sec and a tolerance for exchange of probes of 0.1°C . The meter currently used gives readings to within $\pm 0.3^\circ\text{C}$.

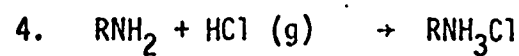
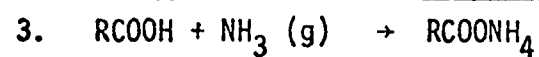
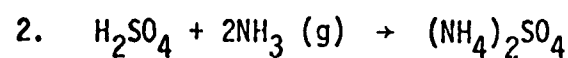
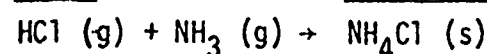
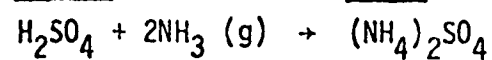
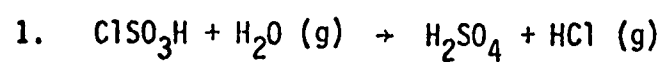
The output of the generator is determined by collection for a period of time, normally 1 min, followed by analysis. The DBP aerosol is collected on a millipore filter ($\sim 1\mu$) and weighed. The acid aerosols are collected in an impinger containing about 100 ml of water and then titrated either coulometrically or with NaOH to a phenolphthalein endpoint. It is also possible, for continuous monitoring, to use a glass pH electrode.

The reactions and reaction conditions employed in this study are given in table 1. The reactions listed are meant only to show the stoichiometry and not to imply anything concerning the extent or sequence of reaction.

2.2 Gas-Aerosol Reactions.

Using the closed reaction tube (figure 1b), emission from all of the reaction systems listed in table 2 was observed. There is an initial rapid jump in emission upon reaction, followed by a slower increase leveling off after about five minutes. Upon cutoff of the reaction gas, the radiometer decrease took place with a half-life also on the order of five minutes. Since the linear flow velocity of the gas-aerosol stream is on the order of 40 cm sec^{-1} , heating of the glass wall of the reaction vessel seemed to be contributing to the emission. This was confirmed by simultaneous radiometer (R) and temperature (T) measurements using the thermistor probe. A plot of R vs T is shown in figure A-3 for the closed tube (figure A-3a). The large

A. Reactions (aerosol underlined)



B. Conditions

1. Flow rates (l/min):

a. sheathing gas, 0.75

b. reactive gas, 0.75

c. aerosol; ClSO_3H , 5.4; all others 3.4

2. Concentrations (g/m^3):

a. NH_3 , 20

b. H_2O , 25

c. HCl , 8

d. aerosol; DBP, 5.1; ClSO_3H , 8.0; H_2SO_4 , 1.0

Aerosol	Gas	ΔH^a	IR ^b
octanoic acid	NH_3	21	w
octylamine	NCl	30	wm
H_2SO_4	NH_3	65	--
	$\text{NH}_3/\text{H}_2\text{O}$	64	m
ClSO_3H	H_2O	0-40 ^c	ms
	$\text{NH}_3/\text{H}_2\text{O}$	96-114 ^c	s

a. Estimated heats of reaction in kcal per mole of aerosol material

b. Indicates infrared emission (w=weak, m=medium, s=strong).

c. Upper figure includes heat of hydration of reaction products.

hysteresis is indicative of wall effects. Nonetheless, the closed tube is still quite useful for screening studies due to its higher sensitivity. For example, there seems to be a rough correlation between the level of infrared emission and the enthalpy of reaction (table 2). The $\text{ClSO}_3\text{H}-\text{H}_2\text{O}$ reaction seems to be an exception, although more quantitative studies are required. These studies may be carried out using an open tube vessel (vide infra).

In order to help eliminate effects due to wall heating, an open tube was employed (figure A-1b). That this system is indeed superior to the closed tube in this regard is shown by the rapid response to the introduction and withdrawal of the reactant gas (figure A-4) and the lack of R vs T hysteresis (figure A-3b). It should be noted that the flow of reactant gas carrier was not changed. The carrier gas could be led through the reactant gas supply or could bypass it. The open tube does suffer from the disadvantage of being more susceptible to external perturbation such as wind currents and vibrations. Note the noise levels in figure A-4. Of course, this was recorded with a 3 sec time constant, and a 100 sec time constant could be used to determine steady-state levels. However, the observed range of measured power per unit area (R) with the open tube is about 1 to $10 \mu\text{W cm}^{-2}$ compared with current "background" levels of about $1 \mu\text{W cm}^{-2}$.

2.3 Temperature-Distance Profiles.

Since it is convenient to determine the fraction of ClSO_3H aerosol reacted in the closed tube, initial measurements of the temperature as a function of distance from the mixing zone were made in this reaction tube. The results are shown in figure A-5. The temperature is measured by the thermistor with the aerosol flowing with and without reactant gas. The quantity ΔT is the difference between these two temperatures. It should be noted that all flow rates are identical since the reactant gas carrier stream

is on but bypassing the aqueous ammonia reservoir. The temperature is constant up to about 10 cm, and then begins to decrease. Since the linear gas velocity is about 100 cm sec^{-1} , this represents a time of 0.1 sec. However, the reaction is not complete at this point, since analysis of the amount of ClSO_3H aerosol reacted at a point about 4 cm further downstream indicates $\leq 85\%$ reaction.

This analysis was performed by passing the gas-aerosol stream through a bed of molecular sieve which passes a majority of the aerosol but no reactant gas. The ClSO_3H aerosol was collected by two impingers in series since previous experience with this material showed that a significant fraction escapes a single impinger, probably due to the formation of HCl . The aqueous solution in each impinger was titrated coulometrically, and followed by monitoring the pH with a glass electrode. The output of the pH meter was displayed on a strip-chart recorder. This result indicates that the reaction rate rapidly slows down. A similar type of behavior was observed by Cadle and Robbins⁸ in the reaction of ammonia with concentrated sulfuric acid droplets (.2 to .9 μm) and ascribed to the diffusion of reaction product in the particle.

Since wall heating effects are known to be present in the closed tube, similar experiments were performed in the open tube. To serve as a basis for comparison, the rate of cooling of a thermally heated dibutyl phthalate (DBP) aerosol was also measured. The results are shown in figure A-6. The ClSO_3H aerosol appears to maintain temperature longer than the heated aerosol, which it should if reaction is occurring. However, the difference is not great. It might be expected that the gas and droplet temperature in the case of the heated DBP aerosol are the same. The question as to what temperature is actually being measured in the case of the reacting aerosol will be addressed

below.

A simple treatment of the rate of heat loss from a flowing stream by conduction and radiation, neglecting the velocity profile in the stream, convection, and the difference in speed between the various layers, predicts an exponential decay of temperature with distance. A plot of $\log \Delta T$ vs x does appear linear for the heated DBP aerosol as shown in figure A-7.

2.4 Emittance-Temperature Profiles.

Over a range of temperatures, the (net) radiant emittance (ΔR) should be proportional to ΔT . Therefore, a number of measurements of ΔR vs ΔT were made using heated DBP aerosol, heated gas, and the ClSO_3H aerosol reaction system. The radiometer response for a heated DBP aerosol is shown in figure A-8. The time lag is greater than for the reaction system due to heating and cooling in the glass reaction tube. It should be noted that when the thermistor probe is in the radiometer field of view, considerably higher readings are obtained.

The radiant emittance-temperature profiles, obtained using the open tube and measured all at a fixed distance from the mixing zone, are shown in figure A-9. The solid line is a least-squares fit of the heated DBP data through the origin, and has a slope ($\Delta R/\Delta T$) of $0.56 \mu W \text{ cm}^{-2} K^{-1}$. This is approximately 5% of blackbody. As expected because the aerosol provides only a small fraction of the mass of the emitting radiation all of which (aerosol and gas) is at the same temperature, heated gas (no aerosol) gives essentially the same result, albeit with slightly more scatter. The $ClSO_3H$ aerosol reaction data, on the other hand, exhibits a great deal of scatter. The corresponding values of $\Delta R/\Delta T$ in figure A-9 are 0.82 (reactant gas on-off) and 0.36 (aerosol on-off) $\mu W \text{ cm}^{-2} K^{-1}$. It was earlier reported, based on a few preliminary measurements, that $\Delta R/\Delta T$ was higher for the reaction system¹⁵ but there is no definitive evidence for this in the more extensive set of data of figure A-9. We assume that for the same reaction conditions (flow rate, concentration, etc.) that the ΔR 's will not depend on which reactant is controlled (on-off), therefore this variation in $\Delta R/\Delta T$ must be attributed to variation in the temperature sensed by the thermistor. This raises the question as to the temperature actually being measured by the thermistor in the case of the gas-aerosol reaction. Where unlike the case of uniform heating of an inert aerosol flow in the oven, the gas temperature may differ from that of the reacting aerosol particles it carries. The rate of the gas-aerosol reaction will likely be liquid phase controlled; i.e., controlled either by the rate of diffusion in the liquid drop or by the bulk reaction rate. Typically, this will involve reaction rates V_S or $3 \times 10^{-7} - 3 \times 10^{-8}$ moles $\text{cm}^{-2} \text{s}^{-1}$ for 1μ drops, although faster rates are possible. Under a simple heat transfer model the aerosol will cool rapidly by conduction to the surrounding air such that a steady-state between the rate of heat generation

by reaction and heat loss by conduction should be rapidly ($\sim 30\mu s$) achieved. Thus, the temperature of the aerosol drops (T_d) and surrounding air in the aerosol cloud (T_c) should be given by

$$T_d = T_c + rV_s H_s / \eta_g. \quad (1)$$

where r , H_s and η_g are the drop radius, heat of reaction, and thermal conductivity of the air, respectively. For the above conditions and a ΔH_s of $100 \text{ kcal mole}^{-1}$, $\Delta T = T_d - T_c$ should only be a few hundredths of a degree. If all of the heat generated warmed up the air mass with no loss, the cloud temperature would rise by about 12°C . However, the actual air temperature will depend upon the rate at which the "cloud" cools in our experimental apparatus. Using the result from figure A-7, maximum air temperatures of about 6°C are estimated. Now, aerosol will collect and react on the probe, some fraction of the heat will be transported away by conduction and radiation, and the remainder will heat up the probe to a temperature higher than the carrier gas temperature.

We have observed drops collected on glass slides under the same reaction flow and concentration conditions do show multiple impingements and "puddling" under the microscope. In addition, it is probable that the drops, impinging on the probe surface, expose more surface area and provide a stationary liquid being exposed to a more rapid, flowing supply of reactant gas. This will lead to a more rapid and complete reaction, heating the probe above the temperature of the gas. In this case the true ΔT for the gas is less than that indicated by the probe, therefore the true value of $\Delta R / \Delta T$ for the ClSO_3H aerosol stream is higher than indicated in the measurements. Since the measured values were comparable to the DBP result, the $\Delta R / \Delta T$ for reacting ClSO_3H aerosol is greater than $\Delta R / \Delta T$ for inert aerosol. For this to occur the drops themselves must be emitting more intensely than the DBP drops which were

known to be at the same temperature as the gas. Consequently this would mean that the drop and cloud temperatures were significantly different, as opposed to the $\Delta T = T_d - T_c$ of a few hundredths of a degree estimated by equation (1). Therefore the simplified physical description leading to equation (1) is not adequate for treating the case of a reacting aerosol particle in this size range.

As expected due to emission from the solid object, values of $\Delta R/\Delta T$ increase if the thermistor is moved to a position within the field of view of the radiometer. Furthermore, ΔR vs ΔT profiles obtained with the thermistor probe centered in the radiometer field of view gave the same value of $\Delta R/\Delta T$ ($1.25 \mu W \text{ cm}^{-2} K^{-1}$) for all three cases with relatively little scatter, as shown in figure A-10. This shows that the measured ΔT does accurately reflect the temperature of the probe itself and that the radiometer responds linearly to the probes greybody emission over the temperature range of these experiments.

3. CONCLUSION

These initial studies have shown that it is possible to observe infrared emission from gas-aerosol reactions and to perform reasonably accurate measurements under controlled conditions. However, many questions remain to be answered before a quantitative model can be developed. In particular, is the drop and cloud (gas) temperature essentially the same or different? How must equation (1) be modified to properly reflect the heat transfer between a reacting drop and the surrounding gas? Future work must involve a study of rate of reaction, heat transfer and radiative emission, as well as a determination of the spectral distribution of the emitted radiation.

REFERENCES

1. "Handbook of Infrared Radiation From Combustion Gases," R. Goulard and J.A.L. Thomson, Eds., Washington Science and Technical Information Office, NASA (1973).
2. R.H. Essenhigh and I Fells, Discuss. Faraday Soc., 30, 208 (1960).
3. P. Mirabel and J.L. Katz, J. Chem. Phys., 60, 1138 (1974).
4. C.J. Shen and G.S. Springer, Atmos. Environ., 10, 255 (1976).
5. H. Reiss, D.I. Margolese and F.J. Schelling, J. Colloid and Interface Sci., 56, 511 (1976).
6. J.P. Friend, Tellus, 18, 465 (1966).
7. M.J. Heard and P.D. Wiffen, Atmos. Environ., 3, 337 (1969).
8. R.D. Cadle and R.C. Robbins, Discuss. Faraday Soc., 30, 155 (1960).
9. R.C. Robbins and R.D. Cadle, J. Phys. Chem., 62, 469 (1958).
10. H.F. Johnstone and D.R. Coughanour, Ind. Eng. Chem., 50, 1169 (1958).
11. A.P. Van den Heuval and B.J. Mason, Quart. J. Roy Meteorol. Soc., 89, 271 (1963).
12. M.D. Carabi, Chem. Soc. Rev., 1, 411 (1972).
13. R.D. Cadle, J. Colloid and Interface Sci., 39, 25 (1972).
14. D. McRae, E. Matijevic and E.J. Davis, J. Colloid and Interface Sci., 53, 411 (1975).
15. R.A. Mackay, "Infrared Emission by an Aerosol Cloud," Final Report, U.S. Army Research Office, October 10, 1980.

APPENDIX
LIST OF FIGURES

- Figure A-1. Gas-aerosol Reaction Tubes.
- Figure A-2. Schematic Diagram of Reaction System.
- Figure A-3. Radiometer reading (R) vs probe temperature (T) for (a) closed tube and (b) open tube (vide text).
- Figure A-4. Radiometer response vs time for the $\text{NH}_3/\text{H}_2\text{O}-\text{ClSO}_3\text{H}$ gas-aerosol reaction system. The introduction and cutoff of reactant gas is denoted by arrows.
- Figure A-5. Temperature change (ΔT) vs distance for the $\text{ClSO}_3\text{H}-\text{NH}_3/\text{H}_2\text{O}$ reaction in the closed tube.
- Figure A-6. Temperature change (ΔT) vs distance for heated DBP aerosol (closed circles) and $\text{ClSO}_3\text{H}-\text{NH}_3/\text{H}_2\text{O}$ reaction (open circles) in the open reaction tube.
- Figure A-7. Log of the temperature change (ΔT) vs distance for the heated DBP aerosol in the open reaction tube.
- Figure A-8. Radiometer reading vs time for a heated DBP aerosol in the open reaction tube. The maximum ΔT is 6 C.
- Figure A-9. Net Radiometer reading (ΔR) vs temperature change (ΔT) for heated DBP (open circles), heated nitrogen (filled circles), and $\text{ClSO}_3\text{H}-\text{NH}_3/\text{H}_2\text{O}$ reaction (half-filled circles). Either the reactant gas (left half-filled) or the aerosol (right half-filled) was turned on and off.
- Figure A-10. Net radiometer reading (ΔR) vs temperature change (ΔT) for heated DBP aerosol (open circles), heated nitrogen (filled circles), and $\text{ClSO}_3\text{H}-\text{NH}_3/\text{H}_2\text{O}$ reaction (half-filled) or the aerosol (right half-filled) was turned on and off. In all cases, the thermistor probe was in the radiometer field of view.

APPENDIX

FIGURES

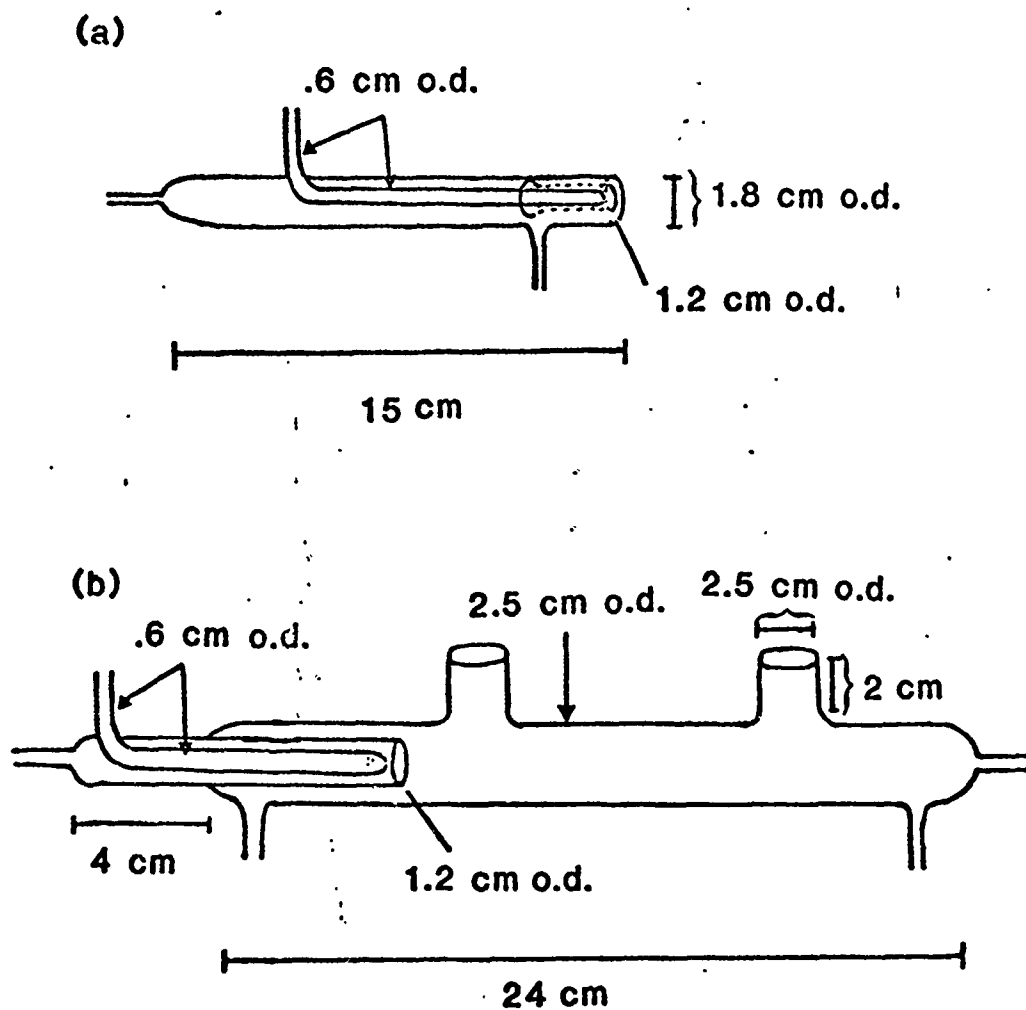


Figure A-1. Gas-aerosol Reaction Tubes

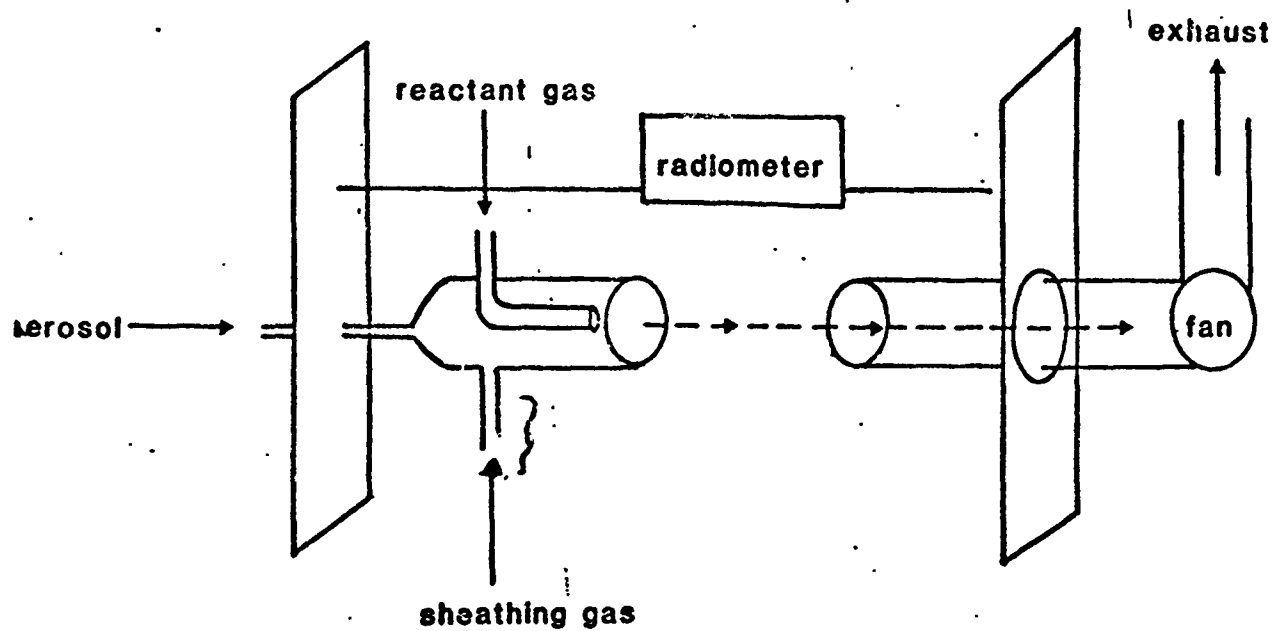
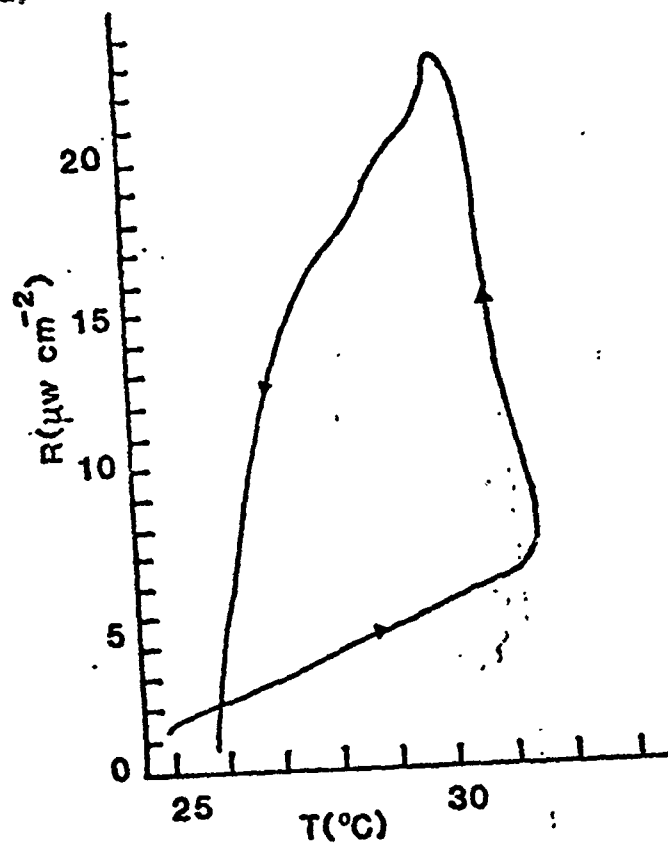


Figure A-2. Schematic Diagram of Reaction System

(a)



(b)

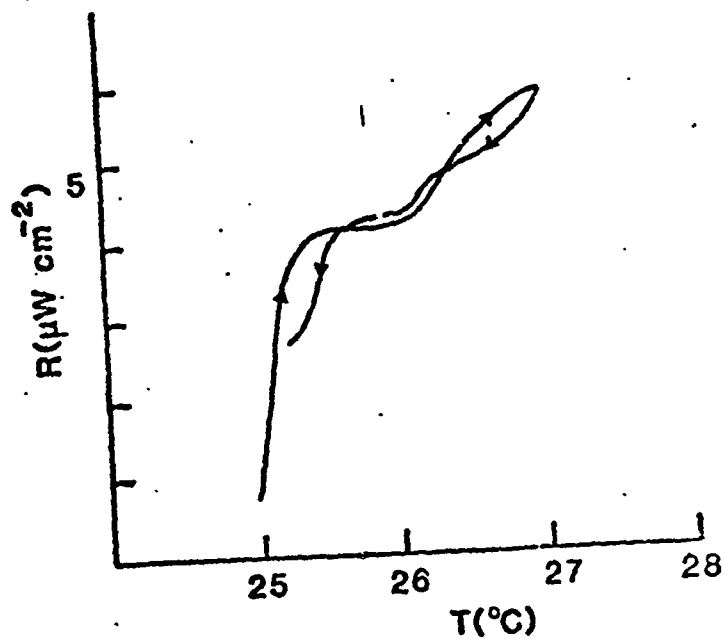


Figure A-3. Radiometer Reading (R) vs probe temperature (T) for (closed tube and (b) open tube (vide text).

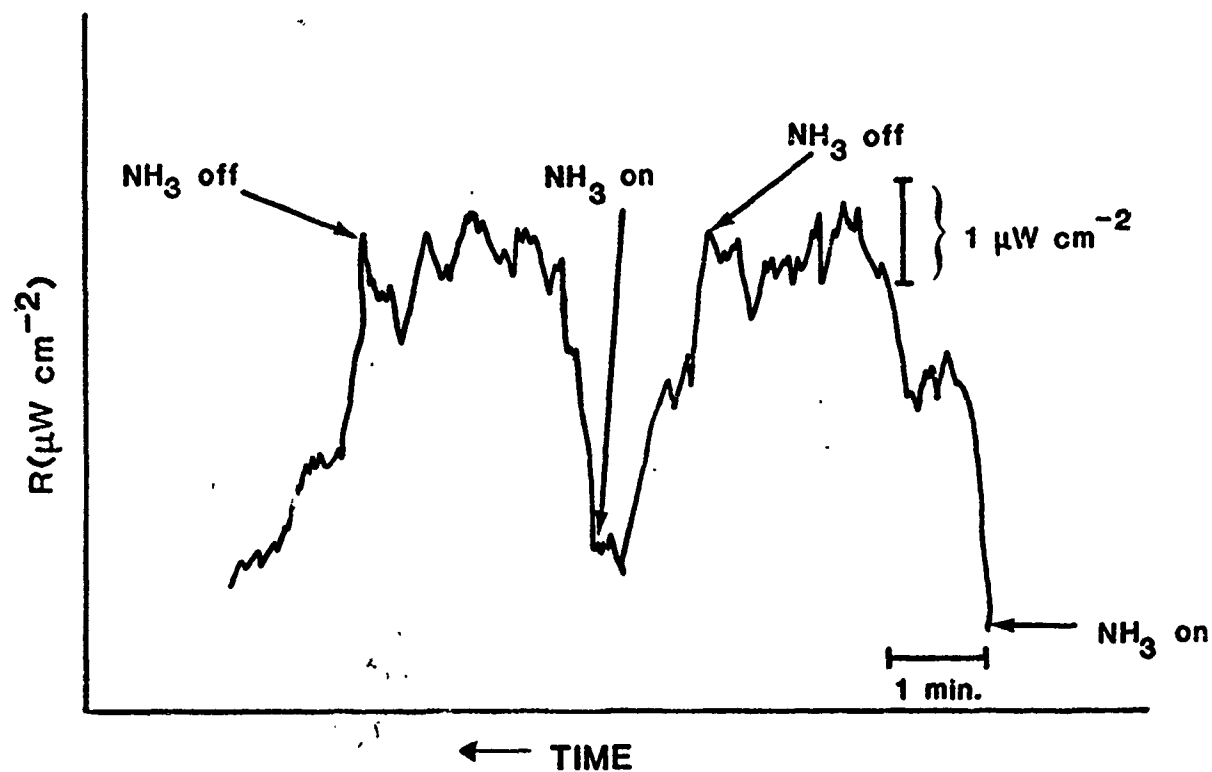


Figure A-4. Radiometer response vs time for the $\text{NH}_3/\text{H}_2\text{O}-\text{ClSO}_3\text{H}$ gas-aerosol reaction system. The introduction and cutoff of reactant gas is denoted by arrows.

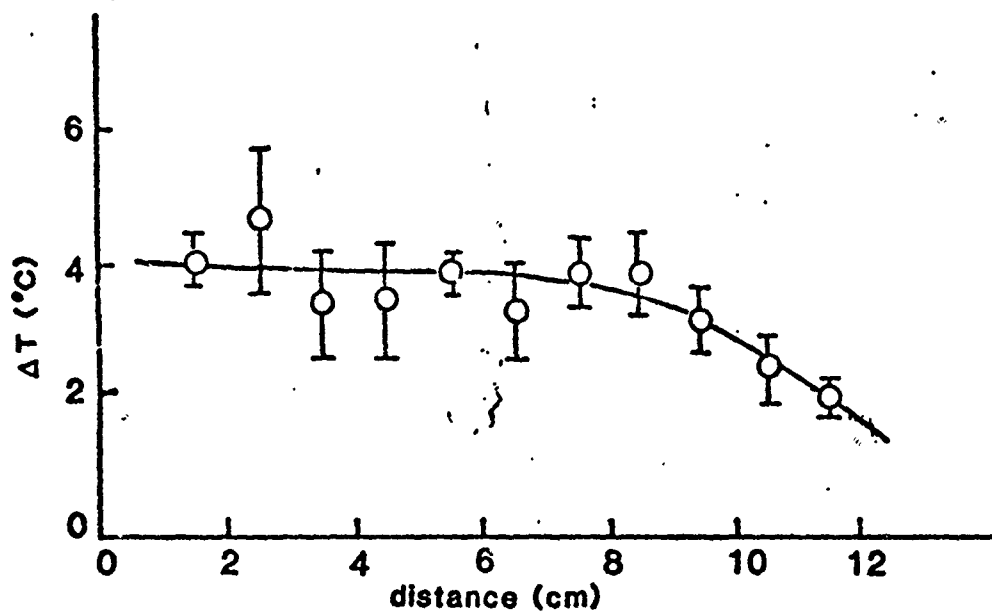


Figure A-5. Temperature change (ΔT) vs distance for the $\text{ClSO}_3\text{H-NH}_3/\text{H}_2\text{O}$ reaction in the closed tube.

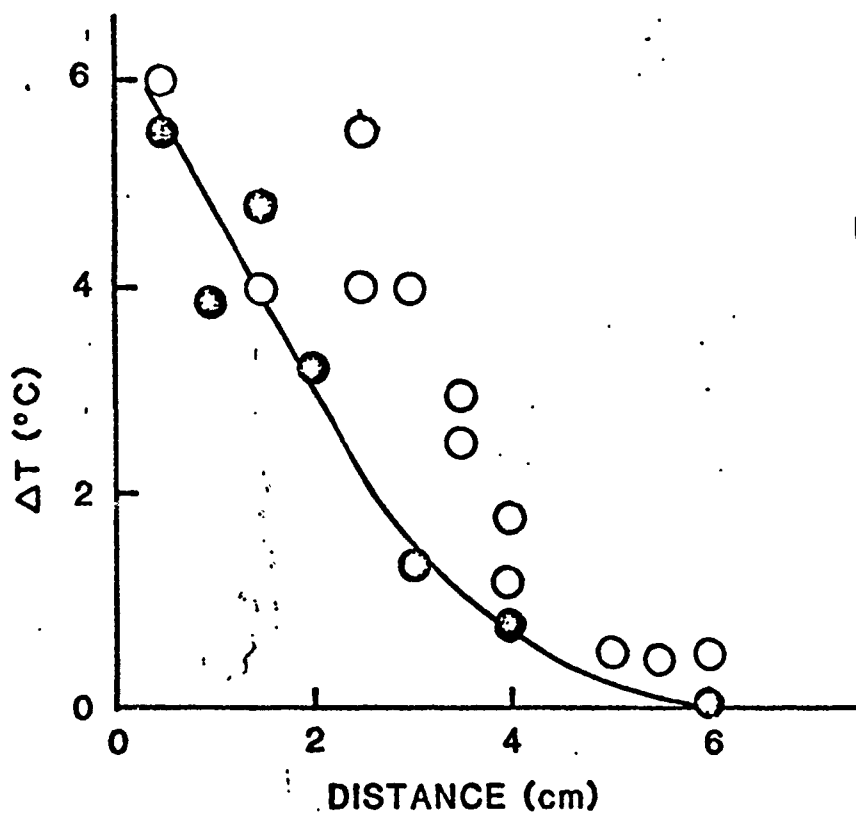


Figure A-6. Temperature change (ΔT) vs distance for heated DBP aerosol (closed circles) and $\text{ClSO}_3\text{H-NH}_3/\text{H}_2\text{O}$ reaction (open circles) in the open reaction tube.

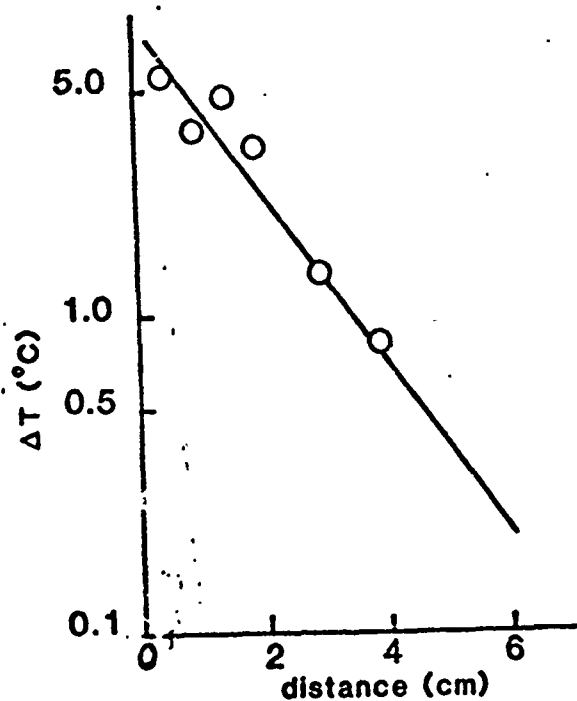


Figure A-7. Log of the temperature change (ΔT) vs distance for the heated DBP aerosol in the open reaction tube.

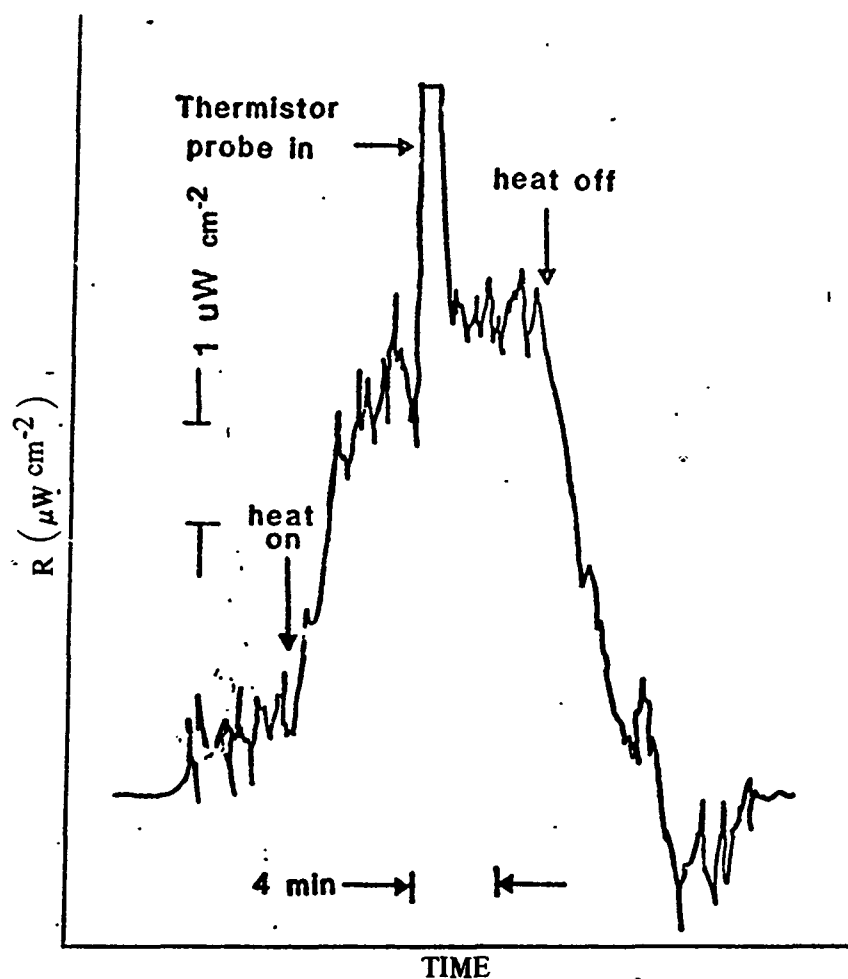


Figure A-8. Radiometer reading vs time for a heated DBP aerosol in the open reaction tube. The maximum ΔT is $6^{\circ}C$.

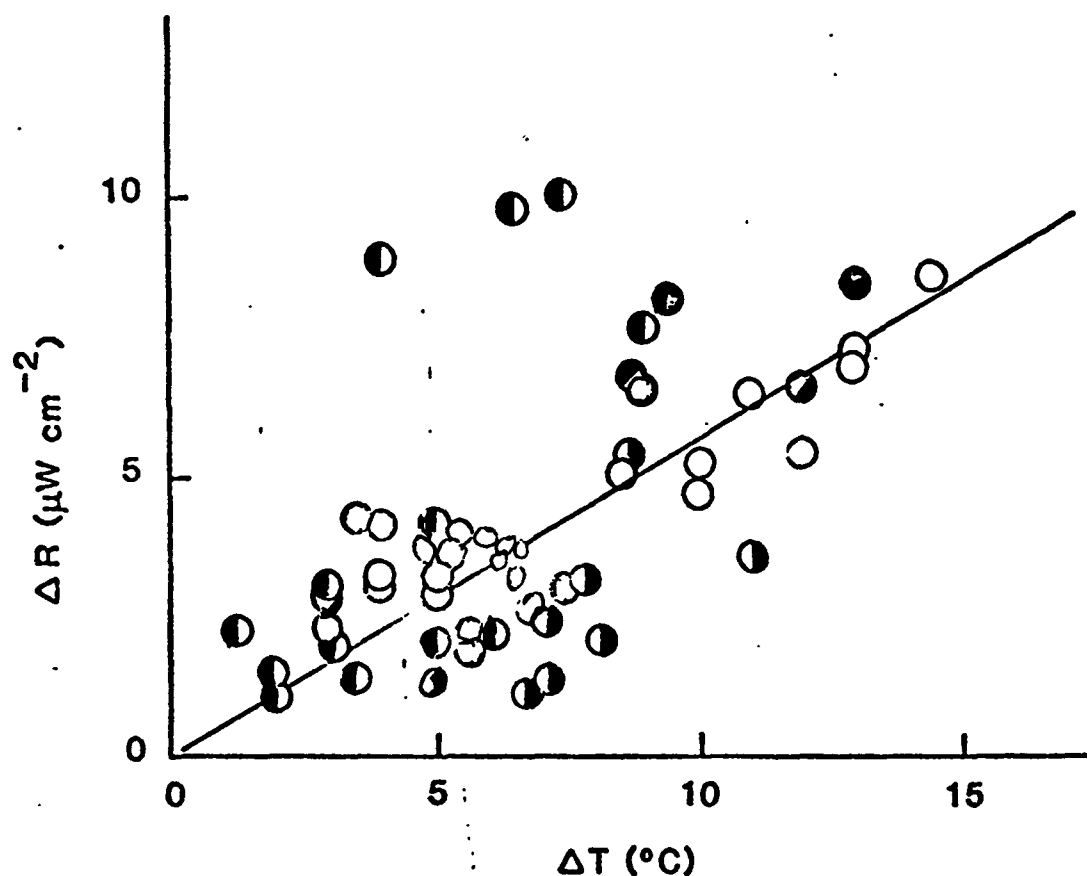


Figure A-9. Net Radiometer reading (ΔR) vs temperature change (ΔT) for heated DBP (open circles), heated nitrogen (filled circles), and ClSO₃H-NH₃/H₂O reaction (half-filled circles). Either the reactant gas (left half-filled) or the aerosol (right half-filled) was turned on and off.

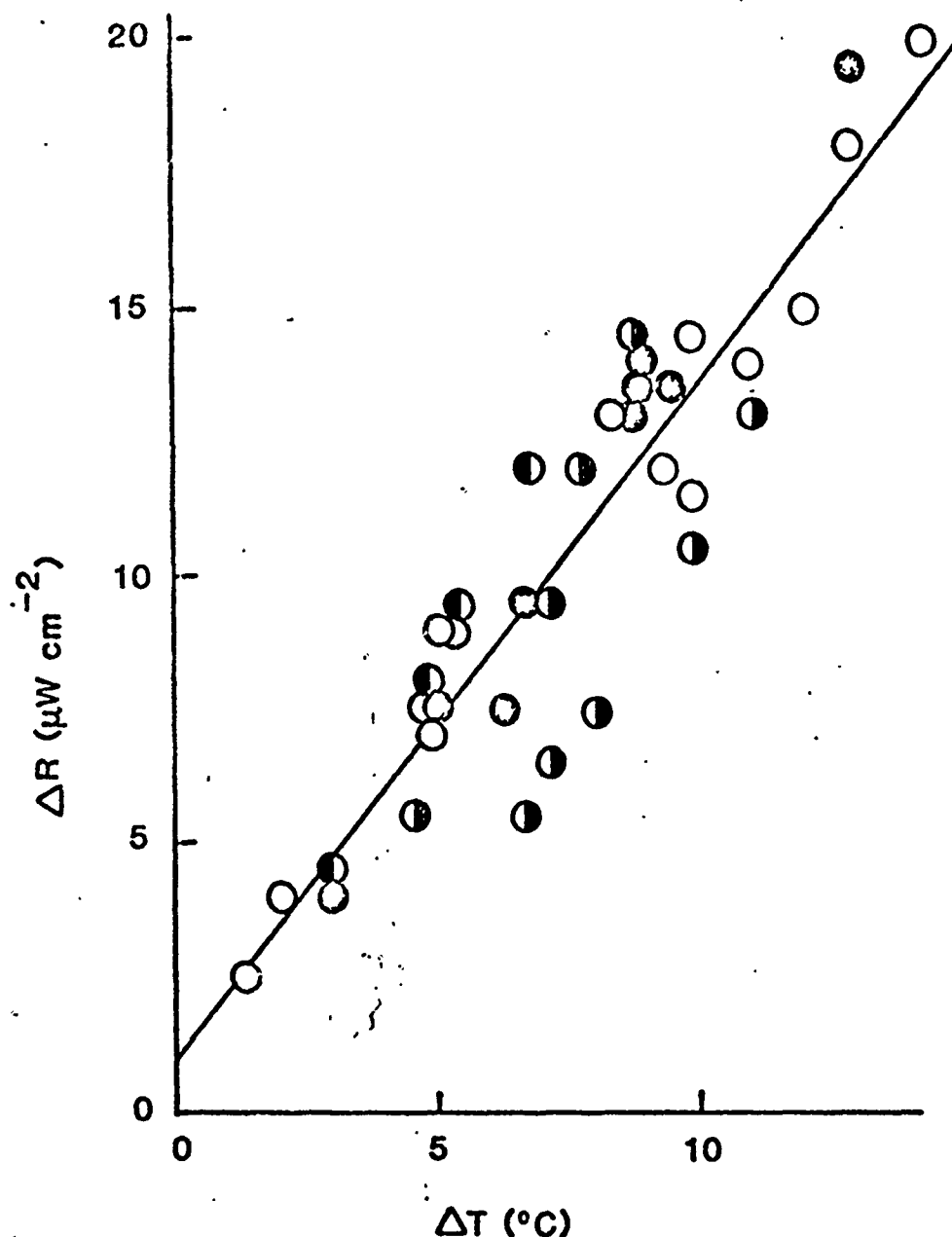


Figure A-10. Net radiometer reading (ΔR) vs temperature change (ΔT) for heated DBP aerosol (open circles), heated nitrogen (filled circles), and $\text{ClSO}_3\text{H-NH}_3/\text{H}_2\text{O}$ reaction (half-filled) or the aerosol (right half-filled) was turned on and off. In all cases, the thermistor probe was in the radiometer field of view.

DISTRIBUTION LIST FOR ARCSL-CR-82028

Names	Copies	Names	Copies
CHEMICAL SYSTEMS LABORATORY			
ATTN: DRDAR-CLB	1	Advanced Research Projects Agency	1
ATTN: DRDAR-CLB-C	1	1400 Wilson Boulevard	
ATTN: DRDAR-CLB-P	1	Arlington, VA 22209	
ATTN: DRDAR-CLB-PS	4	DEPARTMENT OF THE ARMY	
ATTN: DRDAR-CLB-R	1		
ATTN: DRDAR-CLB-T	1	HQDA	
ATTN: DRDAR-CLB-TE	1	ATTN: DAMO-NCC	1
ATTN: DRDAR-CLC-B	1	ATTN: DAMO-NC/COL Robinson (P)	1
ATTN: DRDAR-CLC-C	1	WASH DC 20310	
ATTN: DRDAR-CLF	1		
ATTN: DRDAR-CLJ-R	2	HQDA	
ATTN: DRDAR-CLJ-L	2	Office of the Deputy Chief of Staff for	
ATTN: DRDAR-CLJ-M	1	Research, Development & Acquisition	
ATTN: DRDAR-CLN	1	ATTN: DAMA-CSS-C	1
ATTN: DRDAR-CLN-S	1	Washington, DC 20310	
ATTN: DRDAR-CLN-ST	1		
ATTN: DRDAR-CLT	1	HQ Sixth US Army	
ATTN: DRDAR-CLY-A (Pennsylv. Hundley)	2	ATTN: AFKC-OP-NBC	1
ATTN: DRDAR-CLY-R	1	Presidio of San Francisco, CA 94129	
COPIES FOR AUTHOR(S)			
Research Division	25	Commander	
RECORD COPY: DRDAR-CLB-A	1	DARCOM, STITEUR	
		ATTN: DRXST-STI	1
		Box 48, APO New York 09710	
DEPARTMENT OF DEFENSE			
Defense Technical Information Center		Commander	
ATTN: DTIC-DDA-2	12	USASTCFEO	
Cameron Station, Building 5		ATTN: MAJ Mikeworth	1
Alexandria, VA 22314		APO San Francisco 96328	
Director		Army Research Office	
Defense Intelligence Agency		ATTN: DRXRO-CB (Dr. R. Ghirardelli)	1
ATTN: DB-461	1	ATTN: DRXRO-GS	1
Washington, DC 20301		ATTN: Dr. W. A. Flood	1
		P.O. Box 12211	
		Research Triangle Park, NC 27709	
Deputy Under Secretary of Defense for			
Research and Engineering (R&AT)		HQDA ODUSA (OR)	
ATTN: Dr. Musa	1	ATTN: Dr. H. Fallin	1
ATTN: COL Friday	1	Washington, DC 20310	
ATTN: COL Winter	1		
Washington, DC 20301		HQDA (DAMO-RQD)	
		ATTN: MAJ C. Collat	1
Defense Advanced Research Projects Agency		Washington, DC 20310	
ATTN: Dr. Tegnella	1		
Washington, DC 20301			

HQDA, OCE
ATTN: DAEN-RDM (Dr. Gomez) 1
Massachusetts Ave, NW
Washington, DC 20314

OFFICE OF THE SURGEON GENERAL

Commander
US Army Medical Research and
Development Command
ATTN: SGRD-UBG (Mr. Eaton) 1
ATTN: SGRD-URG-OT (CPT Johnson) 1
ATTN: LTC Don Gensler 1
Fort Detrick, MD 21701

Commander
US Army Medical Bioengineering Research
and Development Laboratory
ATTN: SGRD-UBD-AL, Bldg 568 1
Fort Detrick, Frederick, MD 21701

Commander
USA Medical Research Institute of
Chemical Defense
ATTN: SGRD-UV-L 1
Aberdeen Proving Ground, MD 21010

US ARMY MATERIEL DEVELOPMENT AND READINESS COMMAND

Commander
US Army Materiel Development and
Readiness Command
ATTN: DRCDE-DM 1
ATTN: DRCLDC 1
ATTN: DRCMT 1
ATTN: DRCSF-P 1
ATTN: DRCSF-S
ATTN: DRCDL (Mr. N. Klein) 1
ATTN: DRCBI (COL Gearin) 1
ATTN: DRCBSI-EE (Mr. Giambalvo) 1
ATTN: DRCDMD-ST (Mr. T. Shirata) 1
5001 Eisenhower Ave
Alexandria, VA 22333

Commander
US Army Foreign Science & Technology
Center
ATTN: DRXST-MT3 1
ATTN: DRXST-M73 (Poleski) 1
220 Seventh St., NE
Charlottesville, VA 22901

Director
DARCOM Field Safety Activity
ATTN: DRXOS-SE (Mr. Yutmeyer) 1
Charlestown, IN 47111

PM Smoke/Obscurants
ATTN: DRCPM-SMK-E (A. Van de Wal) 1
ATTN: DRCPM-SMK-M 1
ATTN: DRCPM-SMK-T 1
Aberdeen Proving Ground, MD 21005

Director
US Army Materiel Systems Analysis Activity
ATTN: DRXSY-MP 1
ATTN: DRXSY-CA (Mr. Metz) 1
ATTN: DRXSY-FJ (J. O'Bryon) 1
ATTN: DRXSY-GP (Mr. Fred Campbell) 1
Aberdeen Proving Ground, MD 21005

USA AVIATION RESEARCH AND DEVELOPMENT COMMAND

Director
Applied Technology Lab
USARTL (AVRADCOM)
ATTN: DAVDL-ATL-ASV 1
ATTN: DAVDL-ATL-ASW 1
ATTN: DAVDL-EV-MOS (Mr. Gilbert) 1
Ft. Eustis, VA 23604

Commander
USA Avionics R&D Activity
ATTN: DAVAA-E (M. E. Sonatag) 1
Ft. Monmouth, NJ 07703

USA MISSILE COMMAND

Commander
US Army Missile Command
Director, Energy Directorate
ATTN: DRSMI-RHFT 1
ATTN: DRSMI-RMST 1
ATTN: DRSMI-YLA (N. C. Katos) 1
Redstone Arsenal, AL 35809

Commander
US Army Missile Command
Redstone Scientific Information Center
ATTN: DRSHI-REO (Mr. Widenhofer) 1
ATTN: DRSMI-RGT (Mr. Matt Maddix) 1
ATTN: DRDMI-CGA (Dr. B. Fowler) 1
ATTN: DRDMI-KL (Dr. W. Wharton) 1
ATTN: DRDMI-TE (Mr. H. Anderson) 1
Redstone Arsenal, AL 35809

Commander
US Army Missile Command
Redstone Scientific Information Center
ATTN: DRSMI-RPR (Documents) 1
Redstone Arsenal, AL 35809

USA COMMUNICATIONS-ELECTRONICS COMMAND

Commander
USA Communications-Electronics Command
ATTN: DRSEL-WL-S (Mr. J. Charlton) 1
Ft. Monmouth, NJ 07703

USA ELECTRONICS RESEARCH AND DEVELOPMENT COMMAND

Commander
USA Electronics Research and
Development Command
ATTN: DRDEL-CCM (Dr. J. Scales) 1
ATTN: DELHD-RT-CB (Dr. Sztankay) 1
2800 Powder Mill Road
Adelphi, MD 20783

Commander
Harry Diamond Laboratories
ATTN: DRXDO-RCB (Dr. Donald Wortman) 1
ATTN: DRXDO-RCB (Dr. Clyde Morrison) 1
ATTN: DRXDO-RDC (Mr. D. Giglio) 1
2800 Powder Mill Road
Adelphi, MD 20783

Commander
USA Materials & Mechanics Research Center
ATTN: DRXMR-MDE (Dr. Saul Isserow) 1
Watertown, MA 02172

Commander
USA Cold Region Research Engineering Laboratory
ATTN: George Aitken 1
Hanover, NH 03755

Commander/Director
Combat Surveillance and
Target Acquisition Laboratory
ERADCOM
ATTN: DELCS-R (E. Frost) 1
Ft. Monmouth, NJ 07703

Director

US Army Atmospheric Sciences Laboratory
ATTN: DELAS-AS (Dr. Charles Bruce) 1
ATTN: DELAS-AS-P (Mr. Tom Pries) 1
ATTN: DELAS-EO-EN (Dr. Donald Snider) 1
ATTN: DELAS-EO-EN (Mr. James Gillespie) 1
ATTN: DELAS-EO-ME (Dr. Frank Niles) 1
ATTN: DELAS-EO-ME (Dr. Ronald Pinnick) 1
ATTN: DELAS-EO-MO (Dr. Melvin Heaps) 1
ATTN: DELAS-EO-MO (Dr. R. Sutherland) 1
ATTN: DELAS-EO-S (Dr. Louis Duncan) 1
White Sands Missile Range, NM 88002

US ARMY ARMAMENT RESEARCH AND DEVELOPMENT COMMAND

Commander
US Army Armament Research and
Development Command
ATTN: DRDAR-LCA-L 1
ATTN: DRDAR-LCE-C 1
ATTN: DRDAR-LCU-CE 1
ATTN: DRDAR-NC (COL Fields) 3
ATTN: DRDAR-SCA-T 1
ATTN: DRDAR-SCF 1
ATTN: DRDAR-SCP 1
ATTN: DRDAR-SCS 1
ATTN: DRDAR-TDC (Dr. D. Gyrog) 1
ATTN: DRDAR-TSS 2
ATTN: DRCPM-CAWS-AM 1
Dover, NJ 07801

US Army Armament Research and
Development Command
ATTN: DRDAR-TSE-OA (Robert Thresher) 1
National Space Technology Laboratories
NSTL Station, MS 39529

Requirements and Analysis Office
Foreign Intelligence and Threat
Projection Division
ATTN: DRDAR-RAI-C 1
Aberdeen Proving Ground, MD 21010

Commander
ARRADCOM
ATTN: DRDAR-QAC-E 1
Aberdeen Proving Ground, MD 21010

Director
USA Ballistic Research Laboratory
ARRADCOM
ATTN: DRDAR-BLB 1
ATTN: DRDAR-TSB-S 1
Aberdeen Proving Ground, MD 21005

US ARMY ARMAMENT MATERIEL READINESS
COMMAND

Commander

US Army Armament Materiel Readiness Command

ATTN: DRSAR-ASN 1

ATTN: DRSAR-IRI-A 1

ATTN: DRSAR-LEP-L 1

ATTN: DRSAR-SF 1

Rock Island, IL 61299

Commander

US Army Dugway Proving Ground

ATTN: Technical Library (Docu Sect) 1

Dugway, UT 84022

US ARMY TRAINING & DOCTRINE COMMAND

Commandant

US Army Infantry School

ATTN: CTDD, CSD, NBC Branch 1

Fort Benning, GA 31905

Commandant

US Army Missile & Munitions Center
and School

ATTN: ATSK-CM 1

Redstone Arsenal, AL 35809

Commander

US Army Logistics Center

ATTN: ATCL-MG 1

Fort Lee, VA 23801

Commandant

US Army Chemical School

ATTN: ATZN-CM-C 1

ATTN: ATZN-CM-AD 2

ATTN: ATZN-CN-CDM (Dr. J. Scully) 1

Fort McClellan, AL 36205

Commander

USAAVNC

ATTN: ATZQ-D-MS 1

Fort Rucker, AL 36362

Commander

USA Combined Arms Center and

Fort Leavenworth

ATTN: ATZL-CAM-IM 1

ATTN: ATZL-CA-SAN 1

ATTN: ATZ:-CA-TM-K 1

Fort Leavenworth, KS 66027

Commander

US Army Infantry Center

ATTN: ATSH-CD-MS-C 1

ATTN: ATSH-CD-MS-F 1

ATTN: ATZB-DPT-PO-NBC 1

Fort Benning, GA 31905

Commander

USA Training and Doctrine Command

ATTN: ATCD-N 1

ATTN: ATCD-TEC (Dr. M. Pastel) 1

ATTN: ATCD-Z 1

Fort Monroe, VA 23651

Commander

US Army Armor Center

ATTN: ATZK-CD-MS 1

ATTN: ATZK-PPT-PO-C 1

Fort Knox, KY 40121

Commander

USA TRADOC Systems Analysis Activity

ATTN: ATAA-SL 1

ATTN: ATAA-TDB (L. Dominguez) 1

White Sands Missile Range, NM 88002

Commander

USA Field Artillery School

ATTN: ATSF-GD-RA 1

Ft. Sill, OK 73503

Director

USA Concepts Analysis Agency

ATTN: MOCA-SMC (Hal Hock) 1

8120 Woodmont Avenue

Bethesda, MD 20014

Los Alamos National Laboratory

ATTN: T-DOT, MS 8279 (S. Gerstl) 1

Los Alamos, NM 87545

US ARMY TEST & EVALUATION COMMAND

Commander

US Army Test & Evaluation Command

ATTN: DRSTE-CM-F 1

ATTN: DRSTE-CT-T 1

ATTN: DRSTE-AD-M (Warren Balty) 1

Aberdeen Proving Ground, MD 21005

Commander		Commander	
USA EPG		Naval Surface Weapons Center	
ATTN: STEEP-MM-IS	1	Dahlgren Laboratory	
ATTN: STEEP-MT-DS (CPT Decker)	1	ATTN: DX-21	1
Ft. Huachuca, AZ 85613		ATTN: Mr. R. L. Hudson	1
		ATTN: F-56 (Mr. Douglas Marker)	1
Commander		Dahlgren, VA 22448	
Dugway Proving Ground		Commander	
ATTN: STEDP-MT (Dr. L. Solomon)	1	Naval Intelligence Support Center	
Dugway, UT 84022		ATTN: Code 434 (H. P. St. Aubin)	1
		4301 Suitland Road	
DEPARTMENT OF THE NAVY		Suitland, MD 20390	
Commander		Commander	
Naval Research Laboratory		Naval Explosive Ordnance Disposal	
ATTN: Code 5709 (Mr. W. E. Howell)	1	Technology Center	
ATTN: Code 6532 (Mr. Curcio)	1	ATTN: AC-3	1
ATTN: Code 6532 (Dr. Trusty)	1	Indian Head, MD 20640	
ATTN: Code 6530-2 (Mr. Gordon Stamm)	1	Officer-in-Charge	
ATTN: Code 8320 (Dr. Lothar Ruhnke)	1	Marine Corps Detachment	1
ATTN: Code 8326 (Dr. James Fitzgerald)	1	Naval Explosive Ordnance Disposal	
ATTN: Code 43202 (Dr. Hermann Gerber)	1	Technology Center	
4555 Overlook Avenue, SW		Indian Head, MD 20640	
Washington, DC 20375		Commander	
Chief, Bureau of Medicine & Surgery		Naval Air Development Center	
Department of the Navy		ATTN: Code 2012 (Dr. Robert Helmbold)	1
ATTN: MED 3C33	1	Warminster, PA 18974	
Washington, DC 20372		Commander	
Commander		Naval Weapons Center	
Naval Air Systems Command		ATTN: Code 382 (L. A. Mathews)	1
ATTN: Code AIR-301C (Dr. H. Rosenwasser)	1	ATTN: Code 3882 (Dr. C. E. Dinerman)	1
Washington, DC 20361		ATTN: Code 3918 (Dr. Alex Shlanta)	1
Commander		China Lake, CA 93555	
Naval Sea Systems Command		Commanding Officer	
ATTN: SEA-62Y13 (LCDR Richard Gilbert)	1	Naval Weapons Support Center	
ATTN: SEA-62Y21 (A. Kanterman)	1	Applied Sciences Department	
ATTN: SEA-62Y21 (LCDR W. Major)	1	ATTN: Code 50C, Bldg 190	1
Washington, DC 20362		ATTN: Code 502 (Carl Lohkamp)	1
Project Manager		Crane, IN 47522	
Theatre Nuclear Warfare Project Office		US MARINE CORPS	
ATTN: TN-09C	1	Commanding General	
Navy Department		Marine Corps Development and	
Washington, DC 20360		Education Command	
Institute for Defense Analysis		ATTN: Fire Power Division, D091	1
400 Army-Navy Drive		Quantico, VA 22134	
ATTN: L. Riberman	1		
ATTN: R. E. Roberts	1		
Arlington, VA 22202			

DEPARTMENT OF THE AIR FORCE

HQ AFCL/LOWMM 1
Wright-Patterson AFB, OH 45433

HQ AFSC/SDZ 1
ATTN: CPT D. Riediger
Andrews AFB, MD 20334

USAF TAWC/THL 1
Eglin AFB, FL 32542

USAF SC
ATTN: AD/YQ (Dr. A. Vasiloff) 1
ATTN: AD/YQO (MAJ Owens) 1
Eglin AFB, FL 32542

AFAMRL/TS
ATTN: COL Johnson 1
Wright-Patterson AFB, OH 45433

Commander
Hanscom Air Force Base
ATTN: AFGL-POA (Dr. Frederick Volz) 1
Bedford, MA 01731

Headquarters
Tactical Air Command
ATTN: DRP 1
Langley AFB, VA 23665

AFOSR/NE
ATTN: MAJ H. Winsor 1
Bolling AFB, DC 20332

Dr. Charles Arpke 1
OSV Field Office
P.O. Box 1925
Eglin AFB, FL 32542

OUTSIDE AGENCIES

Battelle, Columbus Laboratories
ATTN: TACTEC 1
505 King Avenue
Columbus, OH 43201

Toxicology Information Center. JH 652
National Research Council 1
2101 Constitution Ave., NW
Washington, DC 20418

Dr. W. Michael Farmer, Assoc.Prof., Physics
University of Tennessee Space Institute 1
Tullahoma, TN 37388

ADDITIONAL ADDRESSEES

Office of Missile Electronic Warfare
ATTN: DELEW-M-T-AC (Ms Arthur) 1
White Sands Missile Range, NM 88002

US Army Mobility Equipment Research and
Development Center
ATTN: DROME-RT (Mr. O. F. Kezer) 1
Fort Belvoir, VA 22060

Director
US Night Vision and EO Laboratories
ATTN: DRSEL-NV-VI (Dr. R. G. Buser) 1
ATTN: DRSEL-NV-VI (Mr. R. Bergemann) 1
ATTN: DELNV-VI (Luanne Obert) 1
ATTN: DELNV-L (D. N. Spector) 1
Fort Belvoir, VA 22060

Commander
217th Chemical Detachment
ATTN: AFVL-CD 1
Fort Knox, KY 40121

Headquarters
US Army Medical Research and
Development Command
ATTN: SGRD-RMS 1
Fort Detrick, MD 21701

Commander
US Army Environmental Hygiene Agency
ATTN: Librarian, Sldg 2100 1
Aberdeen Proving Ground, MD 21010

Commandant
Academy of Health Sciences, US Army
ATTN: HSHA-CDH 1
ATTN: HSHA-IPM 2
Fort Sam Houston, TX 78234